Thermal oscillatory behavior analysis and dynamic modulation of refractive index in microspherical resonator

Quanlong Wang,[1,2] Yue Wang,[1,2] Zhen Guo,[3] Junfeng Wu,[1] and Yihui Wu[1,*]

[1]*State Key Laboratory of Applied Optics, Changchun Institute of Optics, Fine Mechanics and Physics, Chinese Academy of Sciences, Changchun 130033, China*

[2]*University of Chinese Academy of Sciences, Beijing 100039, China*

[3]*Suzhou Institute of Biomedical Engineering and Technology, Chinese Academy of Sciences, Suzhou, Jiangsu 215163, China*

**Corresponding author: yihuiwu@ciomp.ac.cn*

Received January 21, 2015; revised March 6, 2015; accepted March 9, 2015; posted March 11, 2015 (Doc. ID 233048); published March 31, 2015

The thermal nonlinear effects in whispering-gallery-mode resonators are characterized by oscillatory behavior in the transmission spectrum. Although the thermal linewidth broadening is proven to be practical in mode-locking and dynamic control of the optical path, the oscillatory behavior always leads to instability of mode-locking and influences the control accuracy. We theoretically and experimentally illustrate the thermal oscillatory behavior using a model that combines slow and fast thermal relaxation processes of the microsphere and fluctuations of the pump wavelength. We also report dynamic modulation of the refractive index based on the fast thermal relaxation process. © 2015 Optical Society of America

OCIS codes: (140.4780) Optical resonators; (170.4090) Modulation techniques; (190.4870) Photothermal effects; (230.0230) Optical devices.

http://dx.doi.org/10.1364/OL.40.001607

The unique ultrahigh quality factor (Q) and ultrasmall mode volume of a whispering-gallery-mode (WGM) resonator make it a common device for studying light-matter interaction [1–5]. Since the electrical field is intensively enhanced in such an optical microcavity, material absorption will result in obvious thermal nonlinear effects, such as bistability and oscillatory behavior [6,7]. During the thermal nonlinear process, the heat generated by photon absorption dissipates from the mode volume to the rest of the microcavity, i.e., the fast thermal relaxation process, and then from the microcavity structure to the surrounding environment, i.e., the slow thermal relaxation process [6,7]. The thermal effects of the microcavity have garnered much attention [8–13]; in particular, thermal linewidth broadening has already been applied in mode-locking and optical path control [10,11]. However, the thermal nonlinear effects are usually associated with thermal oscillations that jeopardize the mode-locking and the accuracy of optical path control [11,12].

Many factors contribute to thermal oscillations [13,14]. The oscillatory behaviors resulting from mode coupling and Andronov–Hopf bifurcation have been investigated [6,13]. We have observed a type of oscillatory phenomenon in a silica microspherical resonator coupled with a fiber, in which the transmission spectrum only generates downward oscillation peaks in the up-scan of the pump wavelength and upward peaks related to the down-scan process. A similar phenomenon was observed in other laboratories, but the mechanism remains obscure [11].

Here, we demonstrate that a discontinuous sweeping of the pump wavelength and a fast thermal relaxation process result in the oscillatory behavior of the transmission spectrum. Using a thermal dynamical model involving two thermal relaxation processes [7], we investigated the oscillations and obtained results that agree well with the experimental results. With this model, we can also describe dynamic modulation of the refractive index (RI) in the microsphere. We achieved modulation of the RI in the mode volume with frequencies on the order of kilohertz through the fast relaxation process. Although the modulation frequency of thermal process is lower than that of other nonlinear processes, such as the Kerr effect, we can attain a larger modulation range ($\sim 10^{-5}$) owing to the larger thermo-optical coefficient ($dn/dT = 1.2 \times 10^{-5}\ \mathrm{K}^{-1}$) relative to the Kerr coefficient ($2.2 \times 10^{-20}\ \mathrm{m}^2\,\mathrm{W}^{-1}$) [15,16].

The experimental setup is shown in Fig. 1. A digital function generator sweeps the pump wavelength to excite the WGMs in the silica microsphere. We monitor the transmission spectrum in a tapered fiber with an oscilloscope connected to the detector. The Q factor of the microsphere (radius = 125 μm) is $1 \times 10^6 - 1 \times 10^7$ when the input power is sufficiently low to eliminate thermal effects. The entire device is placed in a closed environment and installed on an optical vibration-isolated platform to diminish the influence of airflow, temperature, vibration, and other external disturbances.

The photons coupled into the microsphere are partially absorbed by silica and converted into heat in the mode

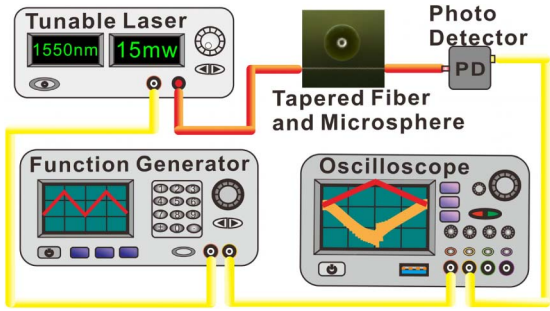

Fig. 1. Schematic representation of the experimental setup.

volume. The heat first dissipates to the rest of the microsphere, and then to the surrounding environment. The temperature difference between the mode volume and the rest of microsphere is denoted as ΔT_1, and the temperature difference between the microsphere structure and the surrounding environment is denoted as ΔT_2. Thus, the total temperature increase of the mode volume ΔT is equal to $\Delta T_1 + \Delta T_2$. The thermo-optical effect leads to an increase in the RI, thereby causing the resonance wavelength to red-shift. When the pump wavelength sweeps in the same direction as the resonance wavelength shift, the resonance linewidth will broaden; when it sweeps in the opposite direction, the resonance linewidth will be compressed, forming the bistability [6]. When the pump wavelength sweeps back and forth periodically on the blue side of the resonance peak, thermal mode-locking can be achieved. Figure 2(a) shows experimental results of thermal mode-locking; the broadened resonance is characterized by the oscillatory behavior. The transmission spectrum directly reflects the relative position between the pump wavelength (λ_p) and the resonance wavelength (λ_r), which is denoted as $\Delta\lambda = \lambda_r - \lambda_p$. Because of the thermal linewidth broadening, the pump light will be long locked in the blue side of a resonance peak, and a slight disturbance of $\Delta\lambda$ will lead to a tremendous fluctuation of the transmission. The total temperature change of the mode volume, ΔT, dominates the shift of λ_r. The first thermal relaxation process only takes tens of microseconds, while the second process takes hundreds of milliseconds for a typical sphere radius of around 125 μm. Therefore, under different sweeping speeds, the two processes have distinct contributions to ΔT. When the pump light changes slowly enough, the fast thermal relaxation process ends instantly. This makes the entire microsphere an isothermal body, in which ΔT_1 approaches zero. Thus, the total temperature change ΔT is dominated by ΔT_2. On the other hand, when the pump light changes too rapidly for the heat to dissipate from the mode volume to the rest of the microsphere, ΔT_1 changes in unison with the pump wavelength, and ΔT_2 undergoes slight change. In this case, ΔT_1 dominates the total temperature change ΔT. The sweeping of the pump wavelength controlled by the function generator is not continuous, because of the instability of the laser and the discontinuous voltage provided from the digital function generator. Therefore, the interaction between the discontinuous change of the pump wavelength and the two thermal relaxation processes causes the fluctuation of $\Delta\lambda$, which leads to the thermal oscillation phenomenon.

In order to describe the thermal oscillatory behavior, we utilized the thermal dynamical equations involving the two thermal relaxation processes [7]. In Eq. (1), the first equation describes the fast thermal relaxation process, and the second equation describes the slow thermal relaxation process. Here C_{p1} is the thermal capacity of the mode volume, C_{p2} is the thermal capacity

$$C_{p1}\Delta\dot{T}_1(t) = I_h \frac{1}{\left(\frac{\lambda_p(t)-\lambda r(t)}{\delta\lambda/2}\right)^2 + 1} - K_1\Delta T_1(t)$$
$$C_{p2}\Delta\dot{T}_2(t) = K_1\Delta T_1(t) - K_2\Delta T_2(t) \quad (1)$$

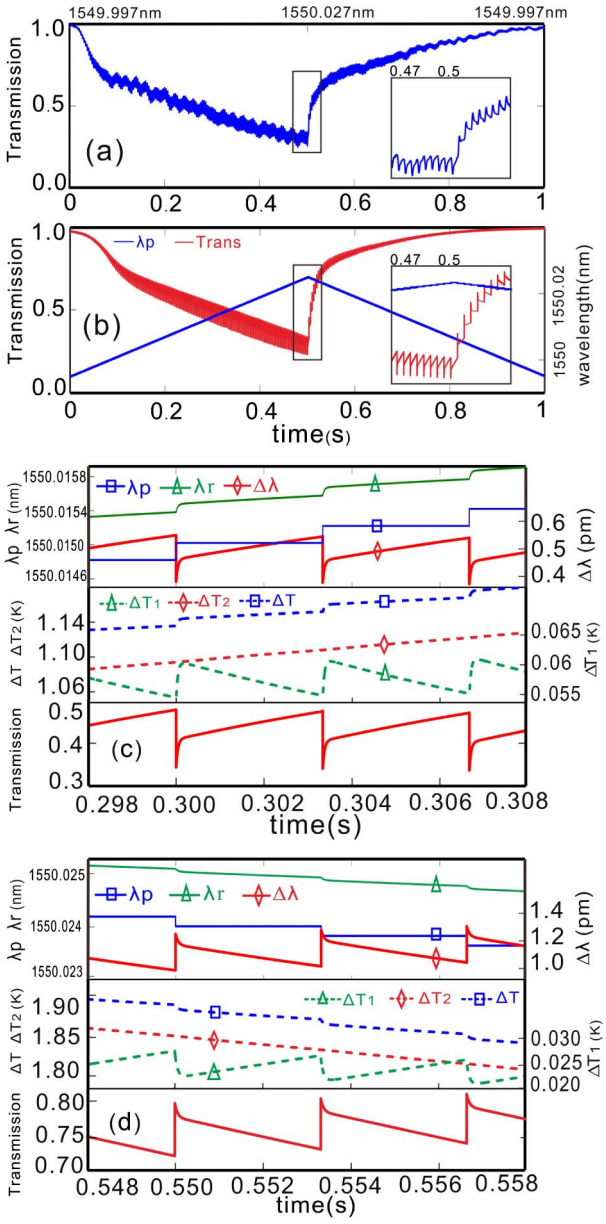

Fig. 2. Thermal oscillatory behavior in the transmission spectra of a microsphere. (a) Experimentally measured transmission spectrum. (b) Calculated results of thermal oscillations. The wavelength is sweeping in the form of steps. (c), (d) Calculated results of the dependence of λ_r, λ_p, ΔT_2, ΔT_1 and transmission on time, with regard to the up-scan and down-scan processes, respectively. The wavelength scan speed v is 0.06 nm/s, and λ_{step} is 2×10^{-4} nm. The measured oscillation period (3.33 ms) is equal to the calculated τ_{step}.

of the microsphere structure, K_1 is the thermal conductivity between the mode volume and the rest of the microsphere, K_2 is the thermal conductivity between the microsphere and the surrounding, $\delta\lambda$ is the resonance bandwidth, and I_h is power of heat generated in cavity when λ_p is in resonance. We assume that the pump wavelength increases or decreases in the form of steps. The duration of each step τ_{step} is equal to λ_{step}/v, where v is the sweeping speed, and λ_{step} is the step of the pump wavelength, whose magnitude could be adjusted by the function generator. Based on this model, the

dependences of λ_r, λ_p, ΔT_2, ΔT_1, and transmission on time are illustrated in Figs. 2(c) and 2(d). The up-scan process and down-scan process are shown in Figs. 2(c) and 2(d), respectively. When the pump wavelength is on the blue side of the resonance, the pump wavelength suddenly steps up toward λ_r, resulting in steep decreases in $\Delta\lambda$ and transmission and an increase in modal power. Meanwhile, the heat generated by absorption increases, leading to a rapid increase in ΔT_1 and a slight and smooth increase in ΔT_2. The total temperature change of the mode volume ΔT rises, pushing λ_r away from λ_p and causes an increase in transmission. The foregoing process creates a downward oscillation peak. When this process occurs repeatedly, a series of downward oscillation peaks can be observed. Inversely, during the down-scan process, the pump wavelength suddenly steps down away from λ_r, resulting in a sharp increase in transmission and a decrease in modal power. Thus, the heat generated in the mode volume decreases, making a sharp decrease in ΔT_1 and a slight and smooth decrease in ΔT_2. The total temperature change of the mode volume ΔT reduces, dragging λ_r toward λ_p. This reduces transmission. Therefore, the increase and the following decrease of the transmission form an upward oscillation peak. Figure 2(b) depicts the modeling result of an entire sweeping period, which agrees well with the oscillation phenomenon that appeared in the experiment. In fact, when sudden changes happen to the pump wavelength, the transmission depends mainly on ΔT_1, for ΔT_2 almost remains unchanged within a short period of time. Thus, each oscillation is dominated by the fast thermal relaxation process. A larger λ_{step} results in a larger amplitude of oscillation. To suppress the oscillation phenomenon, we could adopt a high-resolution function generator to minimize the discontinuity of the output voltage, i.e., minimize the discontinuity of the pump wavelength.

The adjustment of the sweep range can lock the pump wavelength in the same mode during the entire sweeping process [10]. This method has already been applied in the dynamic control of the optical path of probe light [11]. However, this control is influenced by thermal oscillations because of the oscillation having a significant influence on the RI of the mode volume ($\Delta n = \partial n/\partial T \times \Delta T$) [11,12]. Figure 3 shows a modeling result of thermal mode-locking during the entire sweeping process. It is noticeable that ΔT_2 varies in unison with the pump wavelength, while ΔT_1 approaches zero. Therefore, the control of the optical path relies on the slow thermal relaxation process. Thermal oscillations could hardly influence the RI of the rest of the microsphere except for the mode volume ($\Delta n = \partial n/\partial T \times \Delta T_2$). Thus, we could improve the control accuracy by reducing the overlap between the pump light and the probe light modes. The dynamic modulation of the RI of the entire microsphere is limited by the slow thermal relaxation time; the modulation frequency could only reach several Hz [11].

Besides the dynamic modulation, we could also stabilize the RI of the microsphere at a given value. Figure 4 shows the experimental result. Before 3.25 s, the RI of the entire microsphere is modulated in the manner of a triangle wave through the slow thermal relaxation process. After 3.25 s, the pump wavelength maintains a constant

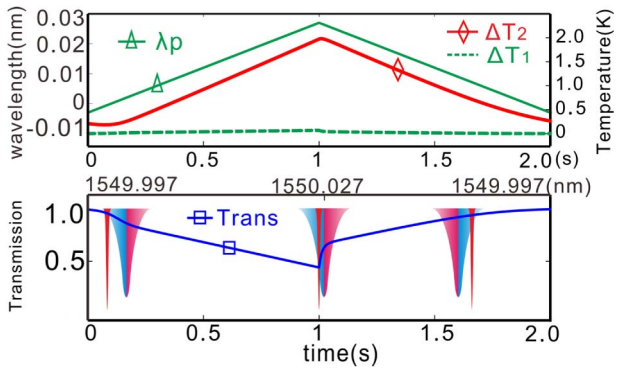

Fig. 3. Thermo-optic locking during one sweeping period. The up panel shows the calculated dependence of λ_p and ΔT_2, and ΔT_1 on time. The down panel gives the calculated transmission spectrum and the relative position between the pump wavelength and the resonance peak at different moments. The sharp red peak denotes the pump wavelength, and the wide peak denotes the resonance peak. During the entire sweeping process, the pump wavelength is on the blue side of the resonance peak.

wavelength output, which leads the microsphere to attain thermal equilibrium. In such a state, the heat generated by absorption in the mode volume is equal to the heat dissipated to the surrounding environment, holding the temperature of the microsphere unchanged and the RI change stabilized at 1.44×10^{-5}.

From the analysis of the thermal oscillation process, we know that the heat does not have enough time to dissipate from the mode volume to the microsphere when the pump wavelength scans quickly. The temperature difference between the mode volume and the rest of the microsphere, ΔT_1, varies in unison with the pump wavelength; the temperature difference between the microsphere structure and the surrounding environment, ΔT_2, almost remains constant. The total temperature change of mode volume relative to the surroundings, ΔT, varies fast with the pump wavelength. Therefore, we could achieve high-frequency modulation of the RI

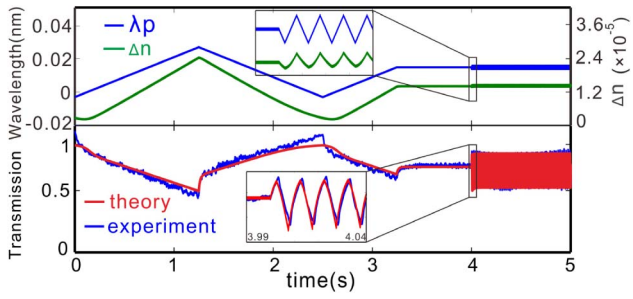

Fig. 4. Dynamic RI modulation in the microsphere. The bottom panel shows the measured and calculated optical transmission spectra. The up panel gives the corresponding dependence of λ_p and Δn on time. Before 3.25 s, the RI of the entire microsphere is modulated at a low frequency of 0.4 Hz. From 3.25 to 4 s, the RI change of the entire microsphere is leveled at 1.44×10^{-5}. After 4 s, the RI of the mode volume is modulated with a high frequency of 100 Hz around 1.44×10^{-5}.

within the mode volume through high-speed sweeping of the pump wavelength. Figure 4 also shows the experimental results of high-frequency modulation after 4 s; the modulation frequency is 100 Hz, but it can reach values as high as tens of kilohertz in experiment. Moreover, modulation in a rectangle wave can also be attained by altering the sweeping manner. Dynamic RI modulation based on the thermal nonlinear effect will have great potential for applications in all-optical devices [17].

In summary, we theoretically and experimentally described thermal oscillatory behavior using the thermal dynamical equations involving the two thermal relaxation processes. The observed behavior is attributed to the combined interaction of the pump wavelength fluctuation and the fast thermal relaxation process. In addition, we achieved dynamic RI modulation of the microsphere. In particular, we achieved high-frequency RI modulation in the mode volume based on the oscillation mechanism. Moreover, we can maintain the RI at a given value for a long period. The dynamic RI modulation described in this work has potential for applications in all-optical devices and could be used to achieve phase-matching in the nonlinear frequency conversion process in a microresonator.

This work was supported by the National Natural Science Foundation of China (Nos. 61102023, 61271139, 51205381, and 11034007), Natural Science Foundation of Jiangsu Province under Grant No. BK20131169, the SRF for ROCS, SEM, and the National High Technology Research and Development Program of China (No. 2012AA040503). We appreciate useful discussion from Jiabin Wu and Chongchong Wang and help from Chang Chen in University of Illinois at Urbana-Champaign.

References

1. K. J. Vahala, Nature **424**, 839 (2003).
2. T. J. Kippenberg, S. M. Spillane, and K. J. Vahala, Phys. Rev. Lett. **93**, 083904 (2004).
3. M. Aspelmeyer, T. J. Kippenberg, and F. Marquardt, *Cavity Optomechanics Nano and Micromechanical Resonators Interacting with Light* (Springer, 2014).
4. S. P. Yu, J. D. Hood, J. A. Muniz, M. J. Martin, R. Norte, C. L. Hung, S. M. Meenehan, J. D. Cohen, O. Painter, and H. J. Kimble, App. Phys. Lett. **104**, 111103 (2014).
5. D. Woolf, P. C. Hui, E. Iwase, M. Khan, A. W. Rodriguez, P. B. Deotare, I. Bulu, S. G. Johnson, F. Capasso, and M. Lončar, Opt. Express **21**, 7258 (2013).
6. V. S. Ilchenko and M. L. Gorodetsky, Laser Phys. **2**, 1004 (1992).
7. T. Carmon, L. Yang, and K. J. Vahala, Opt. Express **12**, 4742 (2004).
8. S. Soltani and A. M. Armani, Appl. Phys. Lett. **105**, 051111 (2014).
9. B. Guha and M. Lipson, Opt. Lett. **40**, 103 (2015).
10. M. Agarwal and I. Teraoka, Appl. Phys. Lett. **101**, 251105 (2012).
11. M. Agarwal and I. Teraoka, Opt. Lett. **38**, 2640 (2013).
12. J. Li, S. Diddams, and K. J. Vahala, Opt. Express **22**, 14559 (2014).
13. A. E. Fomin, M. L. Gorodetsky, I. S. Grudinin, and V. S. Ilchenko, J. Opt. Soc. Am. B **22**, 459 (2005).
14. L. He, Y. F. Xiao, J. Zhu, S. K. Ozdemir, and L. Yang, Opt. Express **17**, 9571 (2009).
15. C. Schmidt, A. Chipouline, T. Pertsch, A. Tünnermann, O. Egorov, F. Lederer, and L. Deych, Opt. Express **16**, 6285 (2008).
16. L. He, Y. F. Xiao, C. Dong, J. Zhu, V. Gaddam, and L. Yang, Appl. Phys. Lett. **93**, 201102 (2008).
17. W. Yoshiki and T. Tanabe, Opt. Express **22**, 24332 (2014).